Photosynthesis Research (2020) 145:43–54
https://doi.org/10.1007/s11120-019-00700-2

ORIGINAL ARTICLE

The topology of plastid inner envelope potassium cation efflux antiporter KEA1 provides new insights into its regulatory features

Bettina Bölter[1] · Melanie J. Mitterreiter[1] · Serena Schwenkert[1] · Iris Finkemeier[2] · Hans-Henning Kunz[3]

Received: 4 July 2019 / Accepted: 11 December 2019 / Published online: 21 December 2019

Abstract

The plastid potassium cation efflux antiporters (KEAs) are important for chloroplast function, development, and photosynthesis. To understand their regulation at the protein level is therefore of fundamental importance. Prior studies have focused on the regulatory K^+ transport and NAD-binding (KTN) domain in the C-terminus of the thylakoid carrier KEA3 but the localization of this domain remains unclear. While all three plastid KEA members are highly conserved in their transmembrane region and the C-terminal KTN domain, only the inner envelope KEA family members KEA1 and KEA2 carry a long soluble N-terminus. Interestingly, this region is acetylated at lysine 168 by the stromal acetyltransferase enzyme NSI. If an odd number of transmembrane domains existed for inner envelope KEAs, as it was suggested for all three plastid KEA carriers, regulatory domains and consequently protein regulation would occur on opposing sides of the inner envelope. In this study we therefore set out to investigate the topology of inner envelope KEA proteins. Using a newly designed antibody specific to the envelope KEA1 N-terminus and transgenic Arabidopsis plants expressing a C-terminal KEA1–YFP fusion protein, we show that both, the N-terminal and C-terminal, regulatory domains of KEA1 reside in the chloroplast stroma and not in the intermembrane space. Considering the high homology between KEA1 and KEA2, we therefore reason that envelope KEAs must consist of an even number of transmembrane domains.

Keywords Chloroplast · Transporter · Protein regulation · Topology · Photosynthesis · Arabidopsis

Introduction

Plastids are eukaryotic cell organelles with diverse metabolic and physiological functions. Although many different specialized plastid types exist in plants, algae, and Apicomplexa they directly or indirectly all originate from an endosymbiotic event between an autotrophic cyanobacterium and a heterotrophic protist cell (Nowack and Melkonian 2010). Eukaryotic photosynthesis takes place exclusively in chloroplasts, which in plants are restricted to the green tissues. The chloroplast has three distinct membranes: an outer and inner envelope membrane, and the thylakoid membrane. Because of its evolutionary history and its central relevance for the cellular metabolism a plethora of transport proteins exist in all three membranes to facilitate selective flux within the organelle and exchange between the plastid and the cytosol (Bölter and Soll 2001; Fischer 2011; Höhner et al. 2016). In the model plant *Arabidopsis thaliana*, three members from the K^+-efflux antiporter (KEA) family reside in the chloroplast: KEA1 and KEA2 in the inner envelope and KEA3 in the thylakoid membrane (Aranda-Sicilia et al. 2012; Armbruster et al. 2014; Kunz et al. 2014). KEA1 and KEA2 are critical for chloroplast function and organelle development (Aranda-Sicilia et al. 2016). Therefore, loss of function in both proteins results in slowly growing Arabidopsis mutants with pale yellow–green leaves (Roston et al. 2012; Kunz et al. 2014). Interestingly, KEA3, which resides

Electronic supplementary material The online version of this article (https://doi.org/10.1007/s11120-019-00700-2) contains supplementary material, which is available to authorized users.

✉ Hans-Henning Kunz
henning.kunz@wsu.edu

[1] Dept. I, Plant Biochemistry, Ludwig Maximilians University Munich, Großhadernerstr. 2-4, 82152 Planegg-Martinsried, Germany

[2] Plant Physiology, Institute of Biology and Biotechnology of Plants, University of Muenster, Schlossplatz 7, 48149 Muenster, Germany

[3] Plant Physiology, School of Biological Sciences, Washington State University, PO Box 644236, Pullman, WA 99164-4236, USA

in the thylakoid membrane, fulfills a very specific role in regulating photosynthesis under dynamic light conditions (Armbruster et al. 2014). Consequently, mutants compromised in KEA3 function display an overall wild-type appearance but reveal a high non-photochemical quenching (NPQ) phenotype upon light shifts (Armbruster et al. 2014; Kunz et al. 2014).

Over the last years, several studies have shown the potential of adjusting photosynthetic efficiency to increase crop yields (Kromdijk et al. 2016; Hubbart et al. 2018). To this end, manipulating the ion flux through chloroplast ion transport proteins represents an interesting avenue to control photosynthesis [reviewed in: (Armbruster et al. 2017)]. However, a recent study on the thylakoid ion transportome revealed that while the membrane localization for the KEA members was confirmed many times, at least some ion transport proteins remain controversial or unknown (Höhner et al. 2019). Therefore, the plastid KEA carriers are a good starting point to manipulate ion and H^+ flux across the chloroplast membranes. To successfully pursue the goal of controlling photosynthesis via plastid ion flux it is not only critical to understand the general mode of action by which KEA carriers function, but it is equally important to elucidate the exact regulatory mechanisms, which govern KEA transport activity.

All plastid KEA proteins share a conserved region in their C-terminus called K^+ transport and NAD-binding (KTN) domain (Roosild et al. 2002). KTN domains have been found in a diverse range of K^+ transport systems. Their close proximity to conserved K^+ channel pores or K^+ transport regions early on suggested an important regulatory role for them. Over the last decades, various studies have revealed that KTN domains can bind $NAD(P)^+$/NAD(P)H (Kröning et al. 2007; Roosild et al. 2009) but also ATP, ADP, and AMP (Johnson et al. 2009; Pliotas et al. 2017). Indeed, the binding of KTN substrates was shown to affect K^+ flux or transport rates of the respective transport proteins.

Thus far, KEA3 is the only family member which has undergone some initial protein topology investigations (Armbruster et al. 2016; Wang et al. 2017). Both studies attempted to pinpoint the suborganellar localization of the C-terminal KTN domain. However so far, the obtained results are unclear and conflicting. Whereas in the initial study thermolysin treatments suggested that the KEA3 KTN domain expands into the thylakoid lumen (Armbruster et al. 2016), later results employing trypsin proposed the opposite, i.e., the KTN domain facing the stromal face of the thylakoid membrane (Wang et al. 2017). Interestingly, both groups and others used a similar in silico model predicting an uneven number of transmembrane (TM) domains for all plastid KEAs (Tsujii et al. 2019). Consequently, the two studies were also inconsistent in the position of the KEA3 N-terminus with either one suggesting opposing faces of the thylakoid membrane as the localization site. Investigating the position of the KEA3 N-terminus is inherently difficult as the soluble stretch is short and after cleavage of the transit peptide unlikely offers sufficient accessible amino acids to design peptide epitopes for antibody production. Therefore, the only experimental data obtained on the KEA3 N-terminus were gathered indirectly by using a pegylation assay and a subsequent small shift in protein size (Wang et al. 2017).

The situation is different for KEA1 and KEA2 (hereafter KEA1(2) if valid for both proteins). While the TM domains between KEA1, KEA2, and KEA3 are highly conserved, exclusively the two envelope carriers possess an approximately 500 amino acids long, soluble N-terminal stretch (Chanroj et al. 2012). Because of this unusual structure, the KEA1/2 N-termini were falsely annotated as separate genes for a long time (Mäser et al. 2001). However, the region is indeed part of a continuous functional reading frame, since T-DNA insertions or loss-of-function mutations in the N-terminus prevent KEA1(2) function (Kunz et al. 2014; Sheng et al. 2014; Luo et al. 2018). Recently, this finding was further corroborated by proteomics showing that KEA1(2) N-termini are subject to post-translational modifications via phosphorylation and acetylation (Reiland et al. 2009; Koskela et al. 2018; Liu et al. 2018). The acetylation is probably catalyzed by the acetyltransferase NSI localized in the chloroplast stroma because *nsi-1* and *nsi-2* loss-of-functions mutants lack acetylation of the KEA1(2) N-termini (Koskela et al. 2018). Although it remains to be shown how acetylation affects transport activity or binding of possible interaction partners, the results suggest that the KEA1(2) N-termini should be exposed to the chloroplast stroma where NSI could access its protein target. However, taking into account the high homology of KEA1(2) with KEA3 throughout their TMs and C-termini, a comparison to the currently suggested odd number of TMs in KEA3 would put the KEA1(2) KTN domain into the IMS preventing a regulatory function on the stromal side.

In summary, to address the open questions regarding the orientation of the regulatory sites of the plastid KEA carriers we sought to investigate the topology of KEA1 and KEA2. To achieve our goal we used trypsin and thermolysin treatments of isolated intact chloroplasts as well as envelope fractions followed by immunoblotting to monitor the protease accessibility of the N-terminus and C-terminus from the two KEA members embedded in the inner chloroplast envelope membrane of *Arabidopsis thaliana*.

Materials and methods

Plant growth

Wild-type (WT) *Arabidopsis thaliana* accession Columbia-0 (Col-0) and mutant seeds were surface sterilized and grown

on ½ Murashige & Skoog (MS) 1% (*w/v*) phytoagar, 1% sucrose plates pH 5.8 for 14 days in 100 µmol photons m^{-2} s^{-1} illumination in a 16/8 h day-night cycle, temperatures 21/18 °C (light/dark). Leaf tissue of 2–3 week old plants was harvested for isolation of total protein extracts or intact chloroplasts.

Single and higher order mutants used in this study

Besides Col-0 WT control plants we employed a number of previously isolated Arabidopsis mutants (all in Col-0 accession background). Loss-of-function T-DNA insertion mutants: *kea1-1* (SAIL_586_D02), *kea2-1* SALK_045324, *kea1-1kea2-1* (SAIL_586_D02, SALK_045324) (Kunz et al. 2014), and *nsi-1* (SALK_033944) (Koskela et al. 2018). As for complementation lines we used: *pUBQ10::KEA1gDNA:YFP* and *pUBQ10::KEA2gDNA:YFP* both expressed in *kea1-1kea2-1* mutant background (Kunz et al. 2014). Proper genetic complementation of photosynthetic phenotypes in *kea1-1kea2-1* + *pUBQ10::KEA1:YFP* and *kea1-1kea2-1* + *pUBQ10::KEA2:YFP* mutant lines was determined using a MAXI version IMAGING-PAM (IMAG-K7 by Walz, Effeltrich, Germany) and the ImagingPAM-Processing toolkit (Schneider et al. 2019).

Generation of *α*-KEA1(2) immunoglobulin

A fragment spanning bp 861–1050 of the *KEA1* cDNA (corresponding to the following peptide:KKDELQKEVD KLNEFAETIQISSLKAEEDVTNIMKLAEQAVAFELEA TQRVNDAEIALQRA) was synthesized with a C-terminal 6xHis-tag and cloned into pMAL-c5x using Sac/HindIII restriction sites (GenScript, Piscataway, USA). The peptide fused to maltose binding protein (MBP) was overexpressed overnight at 18 °C in BL21-CodonPlus (DE3)-RIPL cells (Agilent Technologies, USA). Cells were lysed in lysis buffer (50 mM Tris pH 8.0, 200 mM NaCl) and the fusion protein was bound to Ni–NTA (GE Healthcare) and eluted with lysis buffer containing 250 mM imidazol. The antiserum was raised in rabbits (Biogenes, Berlin, Germany). This serum was purified against heterologously expressed protein transferred to PVDF membrane. The strip was blocked with 5% skim milk in PBS (140 mM NaCl, 2.7 mM KCl, 10 mM Na_2HPO_4, 1.8 mM KH_2PO_4, pH 7.3) for 30 min at RT. The strip was washed three times for 5 min in PBS, then 2 ml of serum were applied followed by incubation at 4 °C overnight. One wash step with PBS + 0.05% Tween 20 was followed by three washings in PBS for 15 min each. Bound antibodies were eluted by applying 100 mM glycine pH 2.6 for 10 min and the eluate was neutralized by addition of 100 mM Tris/HCl pH 8.0. The purified antibody was then incubated with a strip of PVDF membrane with transferred MBP, handled as described above, except that the supernatant after overnight incubation was kept, aliquoted and frozen until further use. In general, all antibodies were raised against heterologously expressed proteins in rabbits. Anti-GFP mouse monoclonal antiserum was obtained from Roche.

Extraction of total leaf proteins and immunoblotting

Leaves were ground in liquid nitrogen and the powder resuspended in an equal volume of 50 mM Tricine pH 8.0, 2% LDS complemented with 1 × complete protease inhibitor (Roche). The mixture was incubated for 30 min on ice and centrifuged at 20.000*g* for 20 min at 4 °C. The supernatant was directly used for protein determination by BCA assay (Pierce), the rest was supplemented with 50 mM EDTA and 10 mM DTT and either directly loaded onto SDS gels or frozen at − 20 °C until further use.

Immunoblotting was performed onto PVDF membranes in Towbin buffer (25 mM Tris pH 8.3, 192 mM glycine, 1% SDS, 20% methanol) in a wet blot apparatus for 1 h at RT at 300 mA or overnight at 4 °C at 60 mA. The membranes were blocked for 30 min with 1% skim milk in 50 mM Tris pH 7.6, 150 mM NaCl, 0.05% Tween 20 (TBS-T) and then incubated with specific antibodies in 1:1000 dilution in TBS-T overnight at 4 °C. Subsequently, membranes were washed three times in TBS-T, then incubated with HRP-coupled secondary antibody (goat-anti-rabbit (Sigma Aldrich) or goat-anti-mouse in case of anti-GFP, respectively) in blocking buffer for 1 h at RT, then washed three times in TBS-T. Proteins were detected by chemiluminescence after incubating the membranes in 100 mM Tris pH 8.5, 25 mM luminol, 4 mM coumaric acid, 0.2% H_2O_2 for 1 min.

Isolation of intact chloroplasts from pea and Arabidopsis

Pea leaves were ground in a kitchen blender in 330 ml isolation medium (330 mM sorbitol, 20 mM MOPS, 13 mM Tris, 3 mM $MgCl_2$, 0.1% (*w/v*) BSA, pH 7.6) and filtered through four layers of mull and one layer of gauze. The homogenate was centrifuged for 1 min at 1500*g* and the pellet was gently resuspended in 1 ml of wash medium (330 mM sorbitol, 50 mM HEPES/KOH, pH 7.6). This suspension was layered onto a discontinuous Percoll gradient of 40/80% Percoll in 330 mM sorbitol, 50 mM HEPES/KOH, pH 7.6 and centrifuged for 5 min at 3000*g* in a swing out rotor. Intact chloroplasts were collected from the 40/80% interface and washed twice with wash medium. The final pellet was resuspended in an appropriate amount of wash medium and the chlorophyll concentration determined (Arnon 1949).

Arabidopsis plants were homogenized by a Polytron mixer in isolation buffer (0.3 M sorbitol, 5 mM $MgCl_2$, 5

mM EDTA, 20 mM HEPES–KOH, 10 mM $NaHCO_3$ pH 8.0) and filtered through one layer of gauze. The filtrate was collected and again mixed in isolation buffer for a total of four times and centrifuged at 1200*g* for 3 min at 4 °C. The pellet was resuspended in residual buffer and layered onto a Percoll gradient (30/82% Percoll in 0.3 M Sorbitol, 20 mM Hepes pH8.0, 5 mM $MgCl_2$, 5 mM EDTA) and centrifuged for 5 min at 1500*g*. Intact chloroplasts were collected from the interface and washed in 50 mM HEPES, 0.3 M sorbitol, 3 mM $MgCl_2$, pH 8.0). The final pellet was resuspended in an appropriate amount of wash medium and the chlorophyll concentration determined (Arnon 1949).

Protease treatments of chloroplasts and inner envelope vesicles

For trypsin treatment of intact chloroplasts an equivalent of 100 µg chlorophyll (chl) was pelleted and resuspended in 100 µl wash buffer supplemented with 0.5 mM $CaCl_2$. Trypsin was added in the indicated amounts per mg chl and incubated for 45 min at 23 °C. The treatment was terminated by addition of 1 × complete protease inhibitor (cpi), chloroplasts were reisolated by centrifugation and washed once with wash buffer + 1 × cpi. The final pellet was solubilized in Laemmli loading buffer containing 2 M urea and 1 × cpi, heated at 65 °C for 5 min and plastids equivalent to 15 µg chl were loaded onto an SDS gel followed by immunoblotting as described above.

Pea chloroplasts were isolated from 20 trays of pea as described above. Intact chloroplasts were lysed by incubation in 0.6 M sucrose, 20 mM tricine, 5 mM EDTA pH 7.6 for 10 min on ice in the dark followed by 50 strokes in a dounce homogenizer. The lysate was diluted 1:2 with 20 mM tricine, 5 mM EDTA pH 7.6 under gentle shaking followed by centrifugation at 5000*g* for 10 min. The supernatant was gently decanted and centrifuged for 1 h at 200,000*g*. The resulting pellet was carefully rinsed with 20 mM tricine, which was then loaded onto sucrose step gradients (0.996 M, 0.800 M and 0.456 M sucrose in 20 mM tricine) and centrifuged at 135,000*g* for 3 h in a swing out rotor. Bands representing the outer and inner envelope vesicles were carefully removed, diluted at least 1:3 with 50 mM NaP_i pH 7.6 and pelleted for 1 h at 135,000*g*. The final pellets were resuspended in 50 mM NaP_i pH 7.6, snap frozen in liquid nitrogen and stored at − 80 °C.

For thermolysin treatment of isolated inner envelope vesicles (Keegstra and Yousif 1986) (see above) equivalent to 10 µg total protein/sample were centrifuged at 256.000*g* for 10 min at 4 °C. The pellet was resuspended in 25 mM HEPES pH 7.6, 5 mM $MgCl_2$, 0.5 mM $CaCl_2$ and 1 µg Thermolysin*10 µg protein^{-1} was added. After 2 min at RT, EDTA was supplemented to a concentration of 10 mM, samples centrifuged as above and the resulting pellet resuspended in 25 mM HEPES pH 7.6, 5 mM EDTA with a subsequent centrifugation step following. The final pellet was resuspended in Laemmli loading buffer containing 2 M urea and 1 × cpi, heated at 65 °C for 5 min and loaded onto an SDS gel followed by immunoblotting.

All experiments were at least done in triplicates giving the same results. Shown here are representative blots.

Topology model of KEA1

The following algorithms were used for the AtKEA1 topology and transmembrane model: Phyre2 web portal for protein modeling, prediction and analysis (Kelley et al. 2015); COILS: Prediction of Coiled Coil Regions in Proteins (Lupas et al. 1991), and TMMOD (Kahsay et al. 2005). For the MW calculation of possible trypsin fragments presented in Table T1 the ProtParam tool provided on the ExPASy server was applied (Gasteiger et al. 2005).

Accession numbers

KEA1 (At1g01790), KEA2 (At4g00630), Tic40 (At5g16620), NSI (At1g32070), Toc64 (At3g17970), Tic62 (At3g18890), Tic55 (At2g24820), FNRL1 (At5g66190).

Identification of PsKEA1(2) was achieved by applying the BLAST function available in the RNA seq database provided by Alves-Carvalho et al. (2015) (http://bios.dijon.inra.fr/FATAL/cgi/pscam.cgi) using the *Pisum sativum* cv. Cameor Low Copy—assembly multi-kmer, library by library. AtKEA1 and AtKEA2 protein sequences were blasted separately.

Results

Design and functional verification of a KEA1/2-specific antibody

To investigate the topology of the plastid inner envelope KEAs and to determine the orientation of their respective soluble N-termini a 61 amino acid peptide, specific to the *Arabidopsis thaliana* carrier KEA1 (Fig. 1a), was heterologously expressed in *E. coli*, purified (Fig. A2a), and injected into rabbits. The resulting antibody was designated α-KEA1(2) because only seven non-consecutive amino acids within the highly conserved N-terminal stretch were found to be different in KEA2 (Fig. 1a, Fig. A1).

For functional verification of the newly designed α-KEA1(2) antibody total leaf protein from Col-0 wild-type plants and loss-of-function mutants *kea1-1*, *kea2-1*, and *kea1-1kea2-1* were extracted. Additionally, we also extracted total leaf protein from *pUBQ10::KEA1(2):YFP* gain of function mutants in the *kea1-1kea2-1* background. The goal here

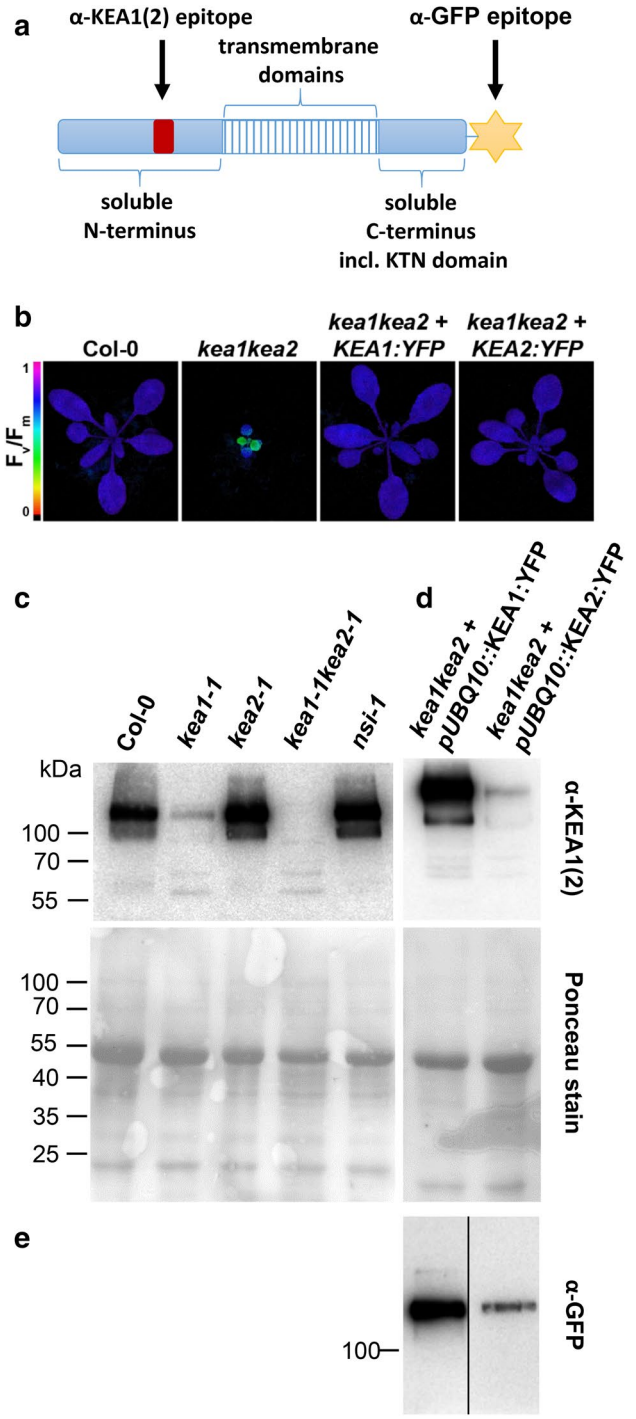

Fig. 1 KEA1 and KEA2 protein expression in different Arabidopsis lines: **a** Schematic representation of KEA1 protein. The peptide against which the antiserum was raised is indicated by a red box, the transmembrane region by a hatched box and the C-terminal YFP protein fusion by a yellow star. **b** False color representation of F_v/F_m in Col-0, *kea1-1kea2-1* double mutant and two complementation lines where native KEA1(2) was replaced by KEA1:YFP or KEA2:YFP, respectively. **c** 20 µg protein of total leaf extract were separated on SDS gels and immunolabeled with α-KEA1(2). **d** The same as in c but membrane exposure time was shortened. Ponceau staining shows equal protein loading. **e** Same leaf extracts from KEA1:YFP and KEA2:YFP were run on a separate gel and probed with α-GFP. Note, the depicted lanes were not directly adjacent on the original membrane as indicated by the vertical black line. Molecular sizes shown on the left

was to introduce a second and independent epitope site on KEA1 and KEA2 that would allow to exclusively probe the C-termini of either protein using a commercial α-GFP antibody (Fig. 1a). As shown by false color images depicting the maximum quantum yield of photosystem II (F_v/F_m) both lines expressed sufficiently high amounts of the respective fusion protein to restore F_v/F_m values to wild-type levels whereas the untransformed *kea1-1kea2-1* control revealed characteristically low F_v/F_m (Fig. 1b). Subsequently, 20 µg of total leaf protein extracts per genotype were separated via SDS page and initially immunoblotted using α-KEA1(2) (Fig. 1c). Whereas the KEA protein was strongly detectable in wild-type controls with a molecular weight of ~ 123 kDa, the KEA-specific signal decreased significantly in *kea1-1* single mutants. Interestingly, the signal in *kea2-1* was slightly stronger than in Col-0 wild-type, which may indicate an upregulation of KEA1 when KEA2 is missing. In the reverse scenario, i.e., in the absence of KEA1 probed with leaf protein extracts from *kea1-1* mutant, KEA2 signal remained well below wild-type level. Notably, in most extracts an additional weak band at ~ 100 kDa was visible (Fig. 1c). This band may represent a degradation product formed during the extraction. As expected, no signal was found when leaf proteins extracted from *kea1-1kea2-1* were decorated with α-KEA1(2). This finding confirms that *kea1-1kea2-1* indeed represents a genuine null mutant. Furthermore, the results show a highly specific binding capacity for α-KEA1(2).

Next, we used protein extracts from *nsi-1* mutants to test if a lack of acetylation on KEA1 and KEA2 would impact the electrophoretic migration and/or protein stability of the proteins as seen in other instances (Buehl et al. 2014). However, no differences in the band size or position were noticeable at the given resolution. Non-acetylated KEA1 and KEA2 proteins were detected equally well and subjectively to similar amounts in leaf protein extract from *nsi-1* mutants (Fig. 1c). These results are in line with the study of Koskela et al. (2018), where a strong decrease in lysine acetylation but no significant protein abundance changes were observed for KEA1 and KEA2 in *nsi* loss-of-function mutants. Lastly, we moved towards testing the second C-terminal epitope site on KEA1 and KEA2 by immunoblotting protein extracts from *pUBQ10::KEA1(2):YFP* overexpressor lines in the *kea1-1kea2-1* mutant background (Fig. 1d). Indeed, α-KEA1(2) recognized the size-shifted, larger fusion proteins in both lines (~ 150 kDa). Notably, although both lines sufficiently expressed KEA1 and KEA2 to fully restore the wild-type phenotype (Fig. 1b), the *pUBQ10::KEA1:YFP* line gave a much stronger signal indicative of higher transgene expression levels in the mutant. Subsequently, this result was confirmed by using a commercial α-GFP antibody detecting the YFP tag on KEA1(2):YFP fusion proteins at the very same size (~ 150 kDa) (Fig. 1e).

Probing the topology of KEA1 N- and C-termini using isolated Arabidopsis wild-type and mutant chloroplasts

Because of its higher expression in leaf tissue, we specifically focused on the topology of KEA1. To this end, intact chloroplasts were isolated from *kea2-1*, *kea1-1kea2-1 + pUBQ10::KEA1:YFP*, *nsi-1*, and Col-0 wild-type plants. Subsequently, plastids were treated with increasing concentrations of trypsin aiming to penetrate only the outer, but not the inner envelope membrane (Jackson et al. 1998). Two controls were employed in the protease treatments: firstly, the outer envelope protein Toc64 (α-Toc64) which is highly susceptible to proteases due to its large cytosolic domain (Sohrt and Soll 2000). Secondly, intactness of the inner envelope membrane in the presence of trypsin was monitored using a Tic40 antibody (Stahl et al. 1999). Tic40 consists of only a very short N-terminal stretch in the intermembrane space (~ 38 amino acids), one transmembrane domain spanning the inner envelope membrane, and the bulk of the protein (detected by α-Tic40) which resides in the stroma (Chou et al. 2003; Froehlich 2011). Thus, disruption of the inner envelope by trypsin results in a rapid loss of α-Tic40 signal due to complete degradation of the Tic40 protein.

The probing of untreated *kea2-1* chloroplasts with α-KEA1(2) resulted in the detection of KEA1 at ~ 123 kDa. Upon trypsin treatment, two stable protein fragments appeared at 100 kDa and 62 kDa (Fig. 2a, indicated by an asterisk and a triangle). A similar pattern was observed for KEA1:YFP fusion proteins in trypsin-treated plastids isolated from *kea1-1kea2-1 + pUBQ10::KEA1:YFP* mutants (100 kDa asterisk and 62 kDa triangle). Additionally, two faint bands, likely representing transitional peptidase products, appeared above and below the 70 kDa marker band (arrow). The main stable 62 kDa (triangle) fragment detected by α-KEA1(2) remained clearly protected from trypsin. This allows to conclude that the KEA1 N-terminus faces the chloroplast stroma, since the antibody only recognizes the N-terminus, as described above. Subsequently, the same membrane was incubated with α-GFP to probe the KEA1 C-terminus. While as expected no signal was observed in extracts from *kea2-1* plastids, distinct signals were detected in lanes with *kea1-1kea2-1 + pUBQ10::KEA1:YFP* mutant chloroplasts (Fig. 2a). After treatment with increasing amounts of trypsin three stable fragments between 100 and 50 kDa accumulated (indicated by diamonds in Fig. 2a). This result strongly indicates that the YFP tag, located at the C-terminus of the protein, is also protected from trypsin and thus must reside in the stroma. Decoration of the same samples with Toc64 antibodies demonstrated the efficiency of the trypsin treatment, i.e., Toc64 signal almost completely vanished resulting from the digestion of the large cytosolic Toc64 domain. In contrast, the vast majority of Tic40 protein remained intact. A very weak degradation product of Tic40 appears in the trypsin-treated samples at approximately 37 kDa, most likely resulting from a few chloroplasts being ruptured during the one hour long treatment and pelleted together with the intact ones. Nevertheless, this result proves the almost complete intactness of the inner membrane throughout the trypsin treatments (Fig. 2a).

To investigate whether the lack of acetylation in the N-terminus has an influence on protease sensitivity for instance due to different folding we treated Col-0 and acetylase deficient *nsi-1* mutant chloroplasts with trypsin. Because an identical band pattern arose from Col-0 and *nsi-1* (100 kDa asterisk and 62 kDa triangle as seen in Fig. 2a) we conclude that KEA1 acetylation does not generally affect protease sensitivity (Fig. 2b).

Finally, to demonstrate that none of the analyzed proteins are intrinsically resistant to trypsin, we incubated chloroplasts with 500 µg trypsin*mg^{-1} Chl in the presence of 1% Triton X-100 (Tx-100). The added detergent resulted in a complete lysis of the chloroplast membranes thereby allowing access of the protease to the stroma. As shown by the lack of immunodetection, all probed proteins were effectively degraded (Fig. 2c).

Probing the localization of the KEA1(2) N-terminus in isolated pea chloroplasts and envelope membrane vesicles

Pea has remained a key system to study the chloroplast proteome and protein import into the organelle. One advantage of pea chloroplasts is that they give access to highly pure fractions of each of the three plastid membranes. Therefore, we were eager to test α-KEA1(2) topology in pea while also verifying our results obtained in Arabidopsis. Indeed, database mining confirmed the presence of KEA1 and KEA2 orthologs in pea on RNA (Alves-Carvalho et al. 2015) and on the proteome level (Gutierrez-Carbonell et al. 2014). BLAST search against this assembled pea transcriptome revealed the presence of two isoforms, Ps020943 and Ps035465. Both show high homology to AtKEA1 and AtKEA2 covering the whole length of the proteins, which is confirmed by peptides identified in proteomics approaches (Fig. A1). Since Ps020943 features a similar high homology score to AtKEA1 than to AtKEA2 and the identified peptides originate from both isoforms, it is difficult to unequivocally assign which of the pea orthologs represents AtKEA1 and AtKEA2, respectively. Comparison of RNA expression levels indicates a higher amount of Ps020943 than Ps035465 RNA, suggesting that the former represents the ortholog to AtKEA1, which is also higher expressed on RNA and on protein level (Fig. 1c). The PsKEA1(2) ortholog was recognized exclusively in the inner envelope fraction from pea

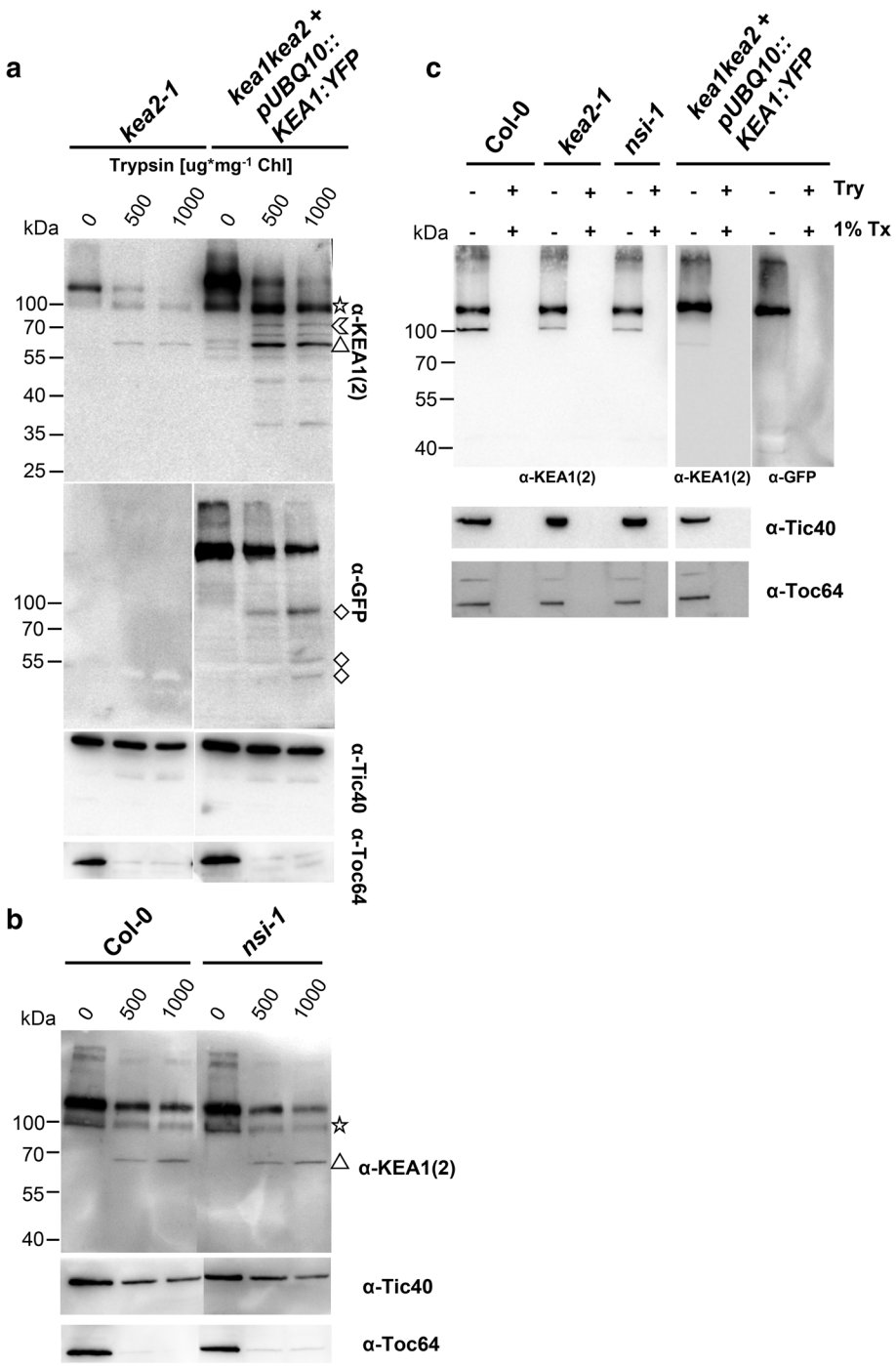

Fig. 2 Trypsin treatment of Arabidopsis chloroplasts: **a** Intact chloroplasts of *kea2-1* and the KEA1:YFP complementation line were treated with 0, 500, or 1000 µg trypsin*mg^{-1} chlorophyll. Samples corresponding to 15 µg chl were separated on SDS gels, transferred onto PVDF and immunolabeled with α-KEA1(2), *α*-GFP, *α*-Tic40, and *α*-Toc64, respectively. Molecular size markers on the left. **b** Intact chloroplasts of Col-0 and *nsi-1* were treated with 0 or 500 trypsin*mg^{-1} chl. Asterisk, arrowhead, triangle and diamond indicate specific KEA1 fragments (for details please refer to the text). *α*-Tic40, and *α*-Toc64 served a trypsin treatment controls

chloroplasts using *α*-KEA1(2) (Fig. 3a). Due to the high identity of AtKEA1 and AtKEA2 in the C-terminal region it is not possible to unequivocally distinguish if pea also features two isoforms. Nevertheless, we performed protease treatments on intact pea chloroplasts as well as isolated inner envelope vesicles from pea to determine if KEA orientation/topology in the inner envelope is conserved across species. In the absence of trypsin, the PsKEA1(2) protein was detected in pea chloroplasts at a similar size to Arabidopsis, i.e., ~ 120 kDa (Fig. 3b). The protein proved to be susceptible to trypsin (Fig. 3b), resulting in three lower molecular weight fragments of approximately 110 kDa, 70 kDa, and 58 kDa, respectively (marked by a black asterisk, arrowhead and triangle), similar to what was observed for Arabidopsis chloroplasts (Fig. 2a–b).

Upon applying high concentrations of trypsin (≥ 500 ng mg^{-1} Chl) the protease gained initial access to the stroma, as indicated by slightly degraded Tic40. Toc64 was again

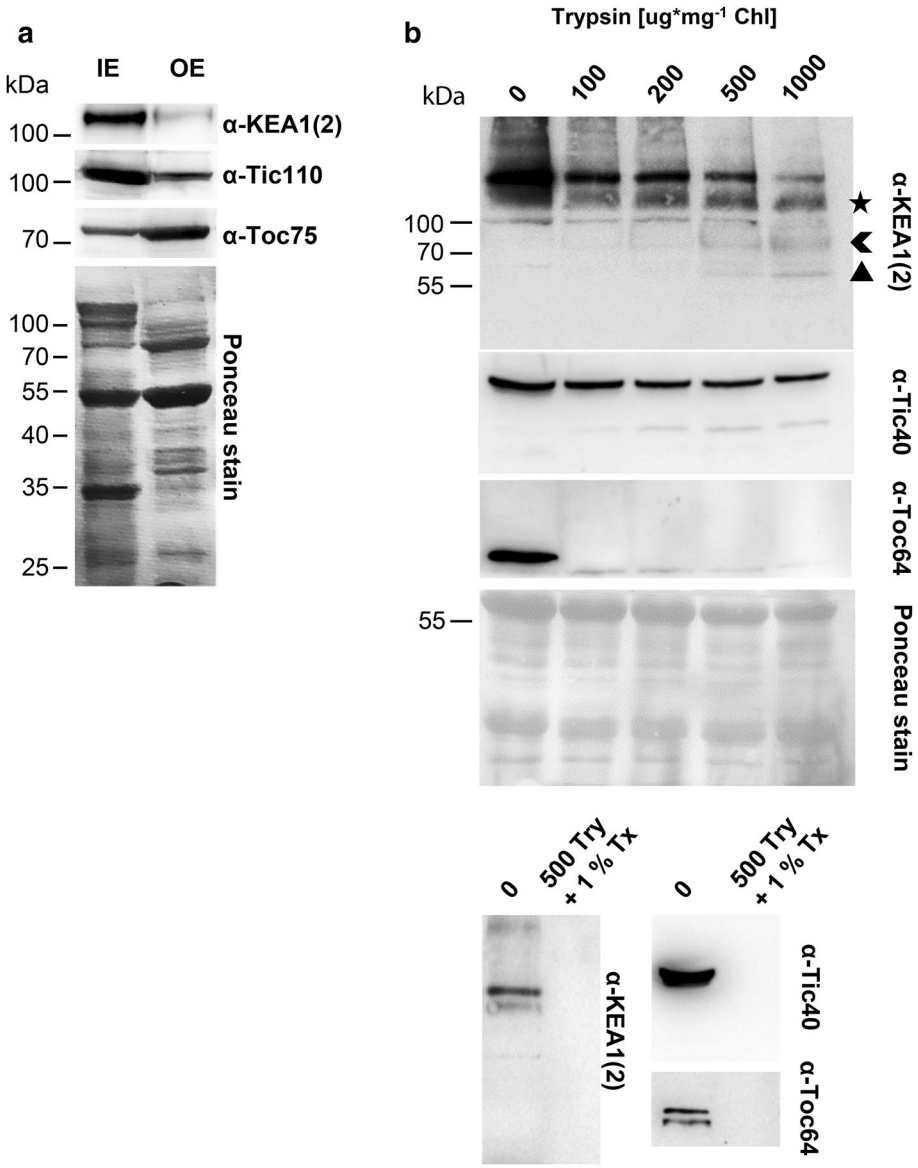

Fig. 3 PsKEA1(2) proteins in pea chloroplasts: **a** Immunoblots of purified outer and inner envelope vesicles from pea chloroplasts, respectively. Membranes equivalent to 10 µg protein were probed with antibodies against KEA1(2), Tic110 as inner and Toc75 as outer envelope control as indicated. The lower panel represents a Ponceau stain of the same membrane. **b** Protease treatments of pea fractions: Intact chloroplasts equivalent to 100 µg chl were treated with 0, 100, 200, 500, or 1000 µg trypsin*mg^{-1} chl. Organelles corresponding to 15 µg chl were separated on SDS gels and probed with the indicated antisera. Asterisk, arrowhead, triangle indicate specific KEA1 fragments. The lower panel shows the Ponceau stain of one representative membrane. Molecular sizes shown on the left. Bottom panels depict trypsin treatment with 500 µg protease in the absence or presence of 1% Tx-100. The membranes were probed with indicated antisera

used as a positive control for trypsin digestion (Fig. 3b). To demonstrate that none of the detected proteins is intrinsically resistant to trypsin, we performed the protease treatment in the presence of 1% Tx-100 as used before on Arabidopsis chloroplasts. As seen in Fig. 3b (bottom panels), KEA, Tic40 as well as Toc64 were completely digested under these conditions. In summary, the results obtained from pea also point to the N-terminus being located in the stroma.

Lastly, we attempted the use of right-side-out isolated inner envelope vesicles (Fig. A2b, c). However, even in the presence of protease inhibitors throughout the isolation the system remained challenging. In the case of the PsKEA1(2) protein and Tic40 some unspecific proteolysis was documented by the presence of lower molecular weight fragments in the samples not treated with protease. Nevertheless, we treated the inner envelopes with thermolysin to elucidate the protease accessibility of the fragments. In this case, thermolysin was chosen over trypsin since it was shown that under the applied experimental conditions it shears off all accessible protein parts without the need for a specific recognition motif which might be buried within the secondary structure and/or by other proteins (Froehlich 2011). Treatments with low concentrations of thermolysin did not compromise the inner envelope membrane integrity as demonstrated by unscathed Tic40 and Tic62, which both reside at the stromal side of the inner membrane. A slight but expected size shift in Tic55, an inner envelope protein with predicted soluble loop in the intermembrane space, was observed. This is consistent with previously obtained data (Caliebe et al. 1997). PsKEA was easily fragmented at the lowest concentration of thermolysin, most likely due to exposed loops in the IMS. Nevertheless, the detection of stable PsKEA1(2) fragments

in the 0.5 or 1 µg thermolysin treated samples confirm the localization of the N-terminus in the stromal compartment.

The fact that these fragments are barely detectable when thermolysin crossed the inner envelope (≥ 2 µg*10 µg^{-1} total protein) as indicated by partly digested Tic40 and a fragment of the stromal protein FNR appearing supports the hypothesis that they are genuine proteolytic products and not unspecifically recognized unrelated pea proteins (Fig. A2c).

A topology model for KEA members in the chloroplast inner envelope membrane

To summarize the data obtained during this study, we generated a topological model of KEA1(2) in which we marked the potentially accessible trypsin cleavage sites located in soluble loops between the predicted transmembrane helices (Fig. 4). Lysine and arginine residues in very small loops and/or extremely close to the membrane were not taken into account since these are usually not recognized by the protease due to their unattainability. From that we deduced the size of expected protease resistant fragments. If all indicated cleavage sites exposed to the IMS were recognized, the N-terminal fragment would be about 67 kDa, whereas the C-terminus including YFP (26.4 kDa) would have an approximate size of 58 kDa. All other resulting fragments would have lost N- and C-terminus and therefore would be undetectable by α-KEA1(2) or α-GFP antibodies. Should only one of the possible recognition sites be cleaved, fragment sizes would be 90 kDa, 82 kDa, 74 kDa, or 67 kDa for the N-terminal part and 58 kDa, 66 kDa, 73 kDa or 80 kDa for the C-terminal end including YFP, respectively. All these numbers are approximations according to the theoretically calculated molecular weight (please refer to Table T1) and do not necessarily exactly represent the apparent running behavior on SDS gels. Taking all this into account, we conclude from the presented data that both N-and C-termini face the stromal side of the inner envelope. We can, however, not absolutely exclude that one or more sites could be protected within the folded protein, though we do not consider this a likely scenario.

Discussion

In this study, we investigated the topology of the chloroplast inner envelope K^+/H^+ exchanger KEA1. A ~ 500 amino acids soluble stretch, exclusively found in inner envelope KEA members, served as an epitope for the design of the antibody α-KEA1(2). This characteristic N-terminal domain is found in KEA1 orthologs from moss, monocots, and dicots (Chanroj et al. 2012). Using chloroplasts isolated from Arabidopsis and pea, we show that α-KEA1(2) can be applied to investigate KEA1(2) expression and protein topology in different plant species. Analysis of isolated chloroplasts in which only KEA1 is present revealed stable N-terminal protein fragments, protected from trypsin. We therefore conclude that the N-terminus of the inner envelope membrane KEAs resides in the chloroplast stroma. In the stroma, the N-terminus becomes acetylated probably by the recently described NSI enzyme (Koskela et al. 2018). Although the biological relevance of KEA1 acetylation requires further research, both findings in conjunction provide initial evidence for a protein–protein interaction, which occurs in the plastid stroma. Inner envelope membrane vesicles isolated

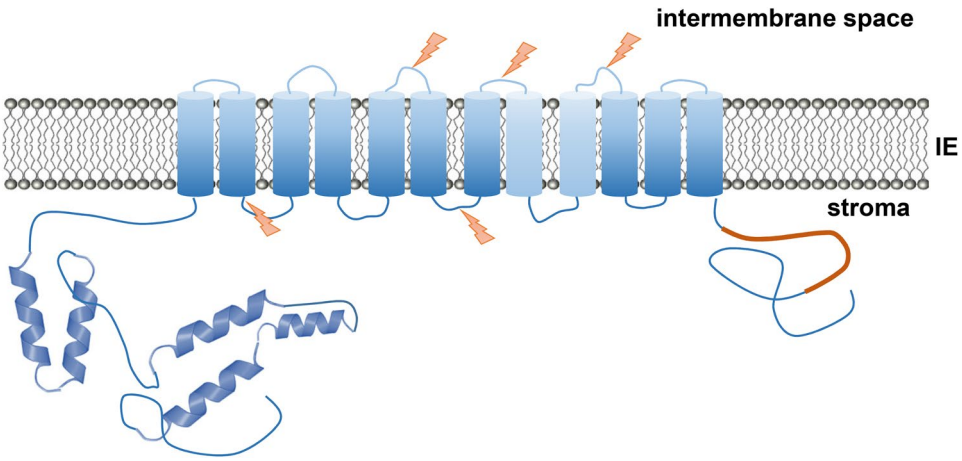

Fig. 4 Topology model of KEA1: Combining our data with structural prediction tools (see M&M), the N-terminal part is predicted to comprise 2–3 coiled coil domains (symbolized by helical structures) and to be oriented towards the stroma. The number of hydrophobic transmembrane alpha helices is not clear – 10 are strongly (blue cylinders), two further are more weakly predicted (light blue cylinders). The C-terminus, containing the KTN domain (orange) also faces the stroma. Possible trypsin recognition sites determined by the protease's known specificity for arginine and lysine residues are symbolized by flashes

from pea chloroplasts strongly favor an right-side-out orientation in aqueous buffers (Waegemann and Soll 1995). This allowed us to confirm the KEA N-terminus localization towards the stroma because proteinase-treated inner envelope vesicles also revealed stable breakdown products recognized by α-KEA1(2).

The second site of potential KEA1 regulation is represented by a KTN domain located in the soluble C-terminal stretch. The same domain is conserved in the C-terminus of the thylakoid carrier KEA3 (Chanroj et al. 2012) where it was shown that the region is required to inhibit thylakoid K^+/H^+ exchange. A truncated KEA3 version lacking the KTN domain seemed more active and had a stronger impact on pH-dependent NPQ induction (Armbruster et al. 2016). In our studies, we found strong evidence that the KTN domain of KEA1 (and thus also likely KEA2) is facing the stromal side of the inner envelope membrane. This assumption is based on our results obtained from functional C-terminal KEA1:YFP fusion proteins and the fact that α-GFP always detected stable KEA1:YFP fragments in trypsin-treated plastids (Fig. 2a).

Because our data indicate localization of N-terminus and C-terminus in the chloroplast stroma, it can be concluded that KEA1 (and likely KEA2) contains an even number of TM domains (Fig. 4). Indeed, a 12 TM domain structure was proposed in the past based on homology modeling of KEA members and their bacterial ortholog KefC (Chanroj et al. 2012). The short soluble KEA3 N-terminus of only seven predicted amino acids after processing of the transit peptide (Sun et al. 2009), has made detailed KEA3 topology studies challenging. However, based on the homology model put forward by Chanroj et al. (2012), it is conceivable that KEA3 also contains 12 TM domains. Additionally, since the transport direction of KEA3 favors pumping of K^+ into the lumen in exchange for protons and under consideration of the KEA1 topology data obtained here, a localization of the KEA3 C-terminal KTN domain in the stroma seems reasonable (Wang et al. 2017). This would allow simultaneous regulation of all three chloroplast KEAs via the KTN domain in the stroma where KTN binding substrates are abundant. The long N-terminus exclusively found in the inner envelope KEAs likely represents a second well-needed layer of protein regulation possibly via lysine acetylation. This two-site regulatory mechanism may be required in physiological conditions in which an independent KEA regulation at the inner envelope and thylakoid membrane is critical. KEA3 plays a role in regulating photosynthesis under dynamic growth light and thus KEA3 activity in the thylakoid membrane needs accurate fine-tuning (Armbruster et al. 2016; Wang et al. 2017; Höhner et al. 2019). However, simultaneously constant K^+/H^+ exchange across the envelope membrane needs to be ongoing to maintain plastid pH and ion homeostasis and with that proper chloroplast function altogether. In line with publicly available transcriptomic data (Fig. A3), our results confirm that KEA1 is far higher expressed in Arabidopsis leaf tissue than KEA2 (Fig. 1c). The fact that *kea1* null mutants remain free of phenotypic malfunction in the greenhouse (Kunz et al. 2014) may indicate that only minute amounts of KEA protein in the chloroplast envelope membrane are sufficient to maintain the physiological function of the organelle under ideal growth conditions. Additionally, the inner envelope KEA proteins may have a very slow turnover, which needs to be addressed in the future.

Acknowledgements Funding: BB DFG, CRC TR175 (B06), SS DFG, CRC 1035 (A04), H-HK NSF Career Award (IOS-1553506), 3rd call ERA-CAPS funding from NSF (IOS-1847382), and (#DE-SC0017160) from DOE. We thank Professor Dr. Jürgen Soll from LMU for supporting this project by initiating the production of α-KEA1(2).

Compliance with ethical standards

Conflict of interest The authors declare that they have no conflicts of interest.

References

Alves-Carvalho S, Aubert G, Carrère S, Cruaud C, Brochot A-L, Jacquin F, Klein A, Martin C, Boucherot K, Kreplak J, da Silva C, Moreau S, Gamas P, Wincker P, Gouzy J, Burstin J (2015) Full-length de novo assembly of RNA-seq data in pea (*Pisum sativum* L.) provides a gene expression atlas and gives insights into root nodulation in this species. Plant J 84:1–19

Aranda-Sicilia MN, Cagnac O, Chanroj S, Sze H, Rodríguez-Rosales MP, Venema K (2012) Arabidopsis KEA2, a homolog of bacterial KefC, encodes a K^+/H^+ antiporter with a chloroplast transit peptide. Biochim Biophys Acta 1818:2362–2371

Aranda-Sicilia MN, Aboukila A, Armbruster U, Cagnac O, Schumann T, Kunz HH, Jahns P, Rodriguez-Rosales MP, Sze H, Venema K (2016) Envelope K^+/H^+ antiporters AtKEA1 and AtKEA2 function in plastid development. Plant Physiol 172:441–449

Armbruster U, Carrillo LR, Venema K, Pavlovic L, Schmidtmann E, Kornfeld A, Jahns P, Berry JA, Kramer DM, Jonikas MC (2014) Ion antiport accelerates photosynthetic acclimation in fluctuating light environments. Nat Commun 5:5439

Armbruster U, Leonelli L, Correa Galvis V, Strand D, Quinn EH, Jonikas MC, Niyogi KK (2016) Regulation and levels of the thylakoid K^+/H^+ antiporter KEA3 shape the dynamic response of photosynthesis in fluctuating light. Plant Cell Physiol 57:1557–1567

Armbruster U, Correa Galvis V, Kunz H-H, Strand DD (2017) The regulation of the chloroplast proton motive force plays a key role for photosynthesis in fluctuating light. Curr Opin Plant Biol 37:56–62

Arnon DI (1949) Copper enzymes in isolated chloroplasts: polyphenoloxidase in *Beta vulgaris*. Plant Physiol. 24:1–15

Bölter B, Soll J (2001) Ion channels in the outer membranes of chloroplasts and mitochondria: open doors or regulated gates? EMBO J 20:935–940

Buehl CJ, Deng X, Liu M, McAndrew MJ, Hovde S, Xu X, Kuo M-H (2014) Resolving acetylated and phosphorylated proteins by neutral urea Triton-polyacrylamide gel electrophoresis: nUT-PAGE. Biotechniques 57:72–80

Caliebe A, Grimm R, Kaiser G, Lubeck J, Soll J, Heins L (1997) The chloroplastic protein import machinery contains a Rieske-type

iron-sulfur cluster and a mononuclear iron-binding protein. EMBO J 16:7342–7350
Chanroj S, Wang G, Venema K, Zhang MW, Delwiche CF, Sze H (2012) Conserved and diversified gene families of monovalent cation/H^+ antiporters from algae to flowering plants. Front Plant Sci 3:25
Chou ML, Fitzpatrick LM, Tu SL, Budziszewski G, Potter-Lewis S, Akita M, Levin JZ, Keegstra K, Li HM (2003) Tic40, a membrane-anchored co-chaperone homolog in the chloroplast protein translocon. EMBO J 22:2970–2980
Fischer K (2011) The import and export business in plastids: transport processes across the inner envelope membrane. Plant Physiol 155:1511–1519
Froehlich J (2011) Studying arabidopsis envelope protein localization and topology using thermolysin and trypsin proteases. In: Jarvis RP (ed) Chloroplast research in arabidopsis: methods and protocols, vol I. Humana Press, Totowa, pp 351–367
Gasteiger E, Hoogland C, Gattiker A, Duvaud Se, Wilki MR, Appel RD, Bairoch A (2005) Protein identification and analysis tools on the ExPASy server. In: Walker JM (ed) The proteomics protocols handbook. Humana Press, Totowa, pp 571–607
Gutierrez-Carbonell E, Takahashi D, Lattanzio G, Rodriguez-Celma J, Kehr J, Soll J, Philippar K, Uemura M, Abadia J, Lopez-Millan AF (2014) The distinct functional roles of the inner and outer chloroplast envelope of pea (*Pisum sativum*) as revealed by proteomic approaches. J Proteome Res 13:2941–2953
Höhner R, Aboukila A, Kunz HH, Venema K (2016) Proton gradients and proton-dependent transport processes in the chloroplast. Front Plant Sci 7:218
Höhner R, Galvis VC, Strand DD, Völkner C, Krämer M, Messer M, Dinc F, Sjuts I, Bölter B, Kramer DM, Armbruster U, Kunz H-H (2019) Photosynthesis in arabidopsis is unaffected by the function of the vacuolar K^+ channel TPK3. Plant Physiol 180:1322–1335
Hubbart S, Smillie IRA, Heatley M, Swarup R, Foo CC, Zhao L, Murchie EH (2018) Enhanced thylakoid photoprotection can increase yield and canopy radiation use efficiency in rice. Commun Biol 1:22
Jackson DT, Froehlich JE, Keegstra K (1998) The hydrophilic domain of tic110, an inner envelope membrane component of the chloroplastic protein translocation apparatus, faces the stromal compartment. J Biol Chem 273:16583–16588
Johnson HA, Hampton E, Lesley SA (2009) The *Thermotoga maritima* Trk potassium transporter—from frameshift to function. J Bacteriol 191:2276–2284
Kahsay RY, Gao G, Liao L (2005) An improved hidden Markov model for transmembrane protein detection and topology prediction and its applications to complete genomes. Bioinformatics 21:1853–1858
Keegstra K, Yousif AE (1986) Isolation and characterization of chloroplast envelope membranes. Methods Enzymol 118C:316–325
Kelley LA, Mezulis S, Yates CM, Wass MN, Sternberg MJE (2015) The Phyre2 web portal for protein modeling, prediction and analysis. Nat Protoc 10:845
Koskela MM, Brünje A, Ivanauskaite A, Grabsztunowicz M, Lassowskat I, Neumann U, Dinh TV, Sindlinger J, Schwarzer D, Wirtz M, Tyystjärvi E, Finkemeier I, Mulo P (2018) Chloroplast acetyltransferase NSI is required for state transitions in *Arabidopsis thaliana*. Plant Cell 30:1695–1709
Kromdijk J, Głowacka K, Leonelli L, Gabilly ST, Iwai M, Niyogi KK, Long SP (2016) Improving photosynthesis and crop productivity by accelerating recovery from photoprotection. Science 354:857–861
Kröning N, Willenborg M, Tholema N, Hänelt I, Schmid R, Bakker EP (2007) ATP binding to the KTN/RCK subunit KtrA from the K^+ -uptake system KtrAB of *Vibrio alginolyticus*: its role in the formation of the KtrAB complex and its requirement *in vivo*. J Biol Chem 282:14018–14027
Kunz HH, Gierth M, Herdean A, Satoh-Cruz M, Kramer DM, Spetea C, Schroeder JI (2014) Plastidial transporters KEA1, -2, and -3 are essential for chloroplast osmoregulation, integrity, and pH regulation in Arabidopsis. Proc Natl Acad Sci USA 111:7480–7485
Liu S, Yu F, Yang Z, Wang T, Xiong H, Chang C, Yu W, Li N (2018) Establishment of dimethyl labeling-based quantitative acetylproteomics in arabidopsis. Mol Cell Proteomics 17:1010–1027
Luo R, Jiang H, Lv Y, Hu S, Sheng Z, Shao G, Tang S, Hu P, Wei X (2018) Chlorophyll deficient 3, encoding a putative potassium efflux antiporter, affects chloroplast development under high temperature conditions in rice (*Oryza sativa* L.). Plant Mol Biol Report 36:675–684
Lupas A, Van Dyke M, Stock J (1991) Predicting coiled coils from protein sequences. Science 252:1162–1164
Mäser P, Thomine S, Schroeder JI, Ward JM, Hirschi K, Sze H, Talke IN, Amtmann A, Maathuis FJM, Sanders D, Harper JF, Tchieu J, Gribskov M, Persans MW, Salt DE, Kim SA, Guerinot ML (2001) Phylogenetic relationships within cation transporter families of arabidopsis. Plant Physiol 126:1646–1667
Nowack ECM, Melkonian M (2010) Endosymbiotic associations within protists. Philos Trans R Soc B 365:699–712
Pliotas C, Grayer SC, Ekkerman S, Chan AKN, Healy J, Marius P, Bartlett W, Khan A, Cortopassi WA, Chandler SA, Rasmussen T, Benesch JLP, Paton RS, Claridge TDW, Miller S, Booth IR, Naismith JH, Conway SJ (2017) Adenosine monophosphate binding stabilizes the KTN domain of the Shewanella denitrificans Kef potassium efflux system. Biochemistry 56:4219–42334
Reiland S, Messerli G, Baerenfaller K, Gerrits B, Endler A, Grossmann J, Gruissem W, Baginsky S (2009) Large-scale arabidopsis phosphoproteome profiling reveals novel chloroplast kinase substrates and phosphorylation networks. Plant Physiol 150:889–903
Roosild TP, Miller S, Booth IR, Choe S (2002) A mechanism of regulating transmembrane potassium flux through a ligand-mediated conformational switch. Cell 109:781–791
Roosild TP, Castronovo S, Miller S, Li C, Rasmussen T, Bartlett W, Gunasekera B, Choe S, Booth IR (2009) KTN (RCK) domains regulate K^+ channels and transporters by controlling the Dimer-Hinge conformation. Structure 17:893–8903
Roston RL, Gao JP, Murcha MW, Whelan J, Benning C (2012) TGD1,-2, and-3 proteins involved in lipid trafficking form ATP-binding cassette (ABC) transporter with multiple substrate-binding proteins. J Biol Chem 287:21406–21415
Schneider D, Lopez LS, Li M, Crawford JD, Kirchhoff H, Kunz H-H (2019) Dynamic light experiments and semi-automated plant phenotyping enabled by self-built growth racks and simple upgrades to the IMAGING-PAM. Plant Methods. https://doi.org/10.1101/795476
Sheng PK, Tan JJ, Jin MN, Wu FQ, Zhou KN, Ma WW, Heng YQ, Wang JL, Guo XP, Zhang X, Cheng ZJ, Liu LL, Wang CM, Liu XM, Wan JM (2014) *Albino midrib 1*, encoding a putative potassium efflux antiporter, affects chloroplast development and drought tolerance in rice. Plant Cell Rep 33:1581–1594
Sohrt K, Soll J (2000) Toc64, a new component of the protein translocon of chloroplasts. J Cell Biol 148:1213–1222
Stahl T, Glockmann C, Soll J, Heins L (1999) Tic40, a new "old" subunit of the chloroplast protein import translocon. J Biol Chem 274:37467–37472
Sun Q, Zybailov B, Majeran W, Friso G, Olinares PDB, van Wijk KJ (2009) PPDB, the plant proteomics database at Cornell. Nucl Acids Res 37:D969–D974
Tsujii M, Kera K, Hamamoto S, Kuromori T, Shikanai T, Uozumi N (2019) Evidence for potassium transport activity of Arabidopsis KEA1-KEA6. Sci Rep 9:10040

Waegemann K, Soll J (1995) Chapter 18 characterization and isolation of the chloroplast protein import machinery. In: Galbraith DW, Bourque DP, Bohnert HJ (eds) Methods in cell biology. Academic Press, Cambridge, MA, pp 255–267

Wang C, Yamamoto H, Narumiya F, Munekage YN, Finazzi G, Szabo I, Shikanai T (2017) Fine-tuned regulation of the K^+/H^+ antiporter KEA3 is required to optimize photosynthesis during induction. Plant J 89:540–553